

OBJECTIVE-PRISM SEARCH OF EMISSION-LINE GALAXIES INSIDE THE HYDRA VOID

CHULHEE KIM

Department of Earth Science Education, Chonbuk National University, Korea

E-mail: chkim@astro.chonbuk.ac.kr

(Received Sep. 11, 2000; Accepted Sep. 18, 2000)

ABSTRACT

In order to identify the candidates of emission-line galaxies inside the southern Hydra Void, photographic objective-prism observations with the UK Schmidt Telescope were carried out using the Tech-Pan films for five fields. All observed prism plates were scanned with the APM Facility and the scanned data was processed to determine the APM plate parameters and to draw spectra. For all galaxy spectra, the emission features, the distance between emission features of $H_{\beta}4861$, $[\text{OIII}]\lambda\lambda 4959, 5007$ and the overlapping by nearby objects were investigated by eyeballing. A total of 7 candidates of emission-line galaxies inside the Hydra Void were identified.

Key words : emission-line galaxies – void – objective-prism search

I. INTRODUCTION

The discovery of a large volume in Bootes that contains no known normal galaxies (Kirshner et al. 1981, 1987), but does contain 27 galaxies (Cruzen et al. 1997), raises questions about the connection between galaxy population density and individual galaxy properties in places far from rich clusters. In addition, interestingly, no galaxy has been found in Coma Void (Tift & Gregory 1988). Also all 27 galaxies are emission-line galaxies (hereafter ELGs) and most of them are not dwarf galaxies, unlike the predictions of theoretical models of galaxy formation in voids (e.g. Dekel and Silk 1986). Recently Kim et al. (2000) have searched for X-ray emission from the 58 galaxies inside the Bootes Void using the ROSAT ALL-SKY Survey (RASS) data as well as ROSAT pointed observations. They have detected X-ray emissions from 9 galaxies. Out of these 9 galaxies, 3 were AGNs and the remaining 6 are probably all ELGs.

The properties of galaxies inhabiting voids have not been studied well, both because of their small numbers and the difficulty of obtaining complete, unbiased samples of these objects. The models of van de Weygaert & van Kampen (1993) and Dubinski et al. (1993) predict a non-uniform distribution of matter in voids. There are indications that such nonuniformities are present in the galaxy distribution in voids (Hoffman et al. 1992; Weistrop 1994).

IRAS-selected Bootes Void galaxies (Strauss & Huchra 1988; Dey, Strauss & Huchra 1990) are likely to be sources of recent star formation activity or nuclear activity. Radio, millimeter, infrared and optical observations of Bootes Void galaxies confirm they are more luminous on average than ELGs at similar redshift and ~40% of Bootes void galaxies exhibit unusual or disturbed morphologies; one-armed, spirals,

interacting pairs, objects with disturbed morphologies (Cruzen et al 1996; Cruzen, Weistrop & Hoopes 1997). The dilemma is how to determine whether these results are due to selection effects or whether they are really indicative of the bright galaxy population in the Bootes Void.

Understanding the nature of emission-line galaxies is, therefore, very important in the construction of a global picture of galaxies and large-scale structure and the properties of AGNs. It is necessary to identify as many galaxies inside voids as possible. To do this we planned the objective-prism search of ELGs inside the southern Hydra Void discovered by Fairall (1988). We selected Hydra Void because this void is close, big, relatively well-defined and also isolated from other voids. We crudely estimated the center of Hydra Void as RA=11h 30m, Dec=-32° and the redshift distance of about 5000 km s⁻¹ with the diameter of less than approximately 4000 km s⁻¹ from the redshift plots by Fairall (1988). Willmer, et al (1995) also confirmed the existence of the Hydra Void on the spatial distribution of galaxies in general direction of the Hydra-Centauria complex and discussed how that distribution relates to other structures located in the volume within 6000 km s⁻¹ of the Local Group.

II. OBSERVATION

Photographic observations of five fields were secured on three nights between February 8 and May 16, 1994 with the United Kingdom Schmidt Telescope (UKST) operating at the Anglo-Australian Observatory in Australia for five fields towards the Hydra Void. The mirror diameter of UKST is 1.83m and the plate scale is 67.12 arcsec/mm. The photographic plate size is 356mm squared or 6.4°x6.4°. Full details are given in the UKST Handbook (1983). The UKST is designed for survey applications, having a large field of view with

Table 1. Log of UK Schmidt observations.

<i>Plate Number^a</i>	<i>Field Number^b</i>	<i>Center^c RA, DEC</i>	<i>Date^d</i>	<i>LST^e</i>	<i>Exp.^f</i>	<i>Q^g</i>
UR15949P	318	10500 -4000	1994-FEB-08	102000	20.0	aR
UR15951P	502	11000 -2500	1994-FEB-10	080100	20.0	a
UR15954P	503	11220 -2500	1994-FEB-10	101200	20.0	bR
UR16095P	439	11300 -3000	1994-MAY-16	110300	20.0	aR
UR16096P	378	11360 -3500	1994-MAY-16	114600	20.0	a

^aRunning number for all UKST plates.

^bESO/SERC Survey field number.

^cEquinox 1950 coordinates of the plate center.

^dUT date of exposure.

^eLocal Sidereal Time of start of exposure.

^fExposure time in minutes.

^gQuality of the plate.

distortion-free images and a fast focal ratio. When used in conjunction with an objective prism, low resolution spectra of all the images in a field can be obtained very efficiently. The resulting prism plates are effective in detecting emission-line galaxies.

Two degree objective-prism and a WG305 filter were used to achieve the medium-dispersion of $830\text{\AA} \text{ mm}^{-1}$ at H_γ although the dispersion is not linear along the wavelength. The resolution of the spectrum is about 18\AA and the wavelength range is from 4550\AA to 6900\AA . The limiting magnitude of the prism plates is about $m_B=16$ mag and the exposure time for all prism plates was 20 min. Usually the magnitude limit of prism plates is two magnitudes fainter than that of the direct plates. We present a log of the observations in Table 1.

Although usually IIIa-J or -F emulsion has been widely used for the photographic search, we decided to try Kodak Technical 4415 Pan (hereafter Tech-Pan) film because we were informed that this film has much better resolution and S/N ratio than IIIa-F emulsion. Tech-Pan film is very cost-effective only $\sim 10\%$ that of glass plates. There are also obvious transportation, storage, and handling benefits. Large numbers can be shipped cheaply and quickly. The ester-base itself is extremely stable, having excellent strength, toughness and flexibility. Also Tech-Pan film does not suffer the same batch to batch variations as Kodak spectroscopic emulsions on glass. Finally the hypered product stores extremely well in an inert atmosphere in cold storage with no apparent degradation in fog levels with long (~ 1 month) storage times (see Kodak publication Q-34, 1977).

It has been proven by Phillipps & Parker (1993) that Tech-Pan film is extremely successful. The film offers significant gains in depth, resolution, and S/N ratio when compared with conventional photographic film. Also the spectral sensitivity is reasonably flat while the reciprocity failure of the hypered emulsion

is extremely low, an important factor for long exposures. Deep, sky-limited photographs with excellent image quality and resolution have been obtained in a new survey of low surface brightness galaxies in the Virgo Cluster (Schwartzberg, et al 1995).

However Tech-Pan film is proving difficult to copy and needs careful mounting for proper scanning with a measuring machine. Film also tends to pick up dust easily and so needs proper storage and cleaning and longer development times are required. The film can 'kink' so it still requires careful handling. Finally more halation effects are seen with bright images than with IIIa-F.

Table 1 summarizes the properties of the observed prism plate material used in each of the five fields. Column 1 and 2 are the UKST field designation and the plate number. Column 3, 4, 5, and 6 are the coordinates of the field center, the dates of exposure, and local sidereal time of the start of exposure respectively. Column 7 is the exposure time and column 8 is the quality grade of the plate. The first letter of the grade indicates the overall quality of the plate and details of the codes are given in the UKST Handbook (1983).

III. DISCUSSION AND RESULTS

The scanning of the prism plate is performed by the APM (Automatic Plate Measuring) Microdensitometer operating in the Royal Greenwich Observatory with the resolution of 20 microns. A full description is given in the APM Handbook (1981).

The objective-prism spectra of all the objects in the direct plate catalogue constitute the sample to be processed in order to identify ELGs. The initial process is identifying all objects on the prism plate using a similar algorithm as the one employed in DAOFIND to identify all objects. The difference is, in case of the prism plate, instead of circle, a rectangular box is used and the intensity of the head part of the spectrum are searched.

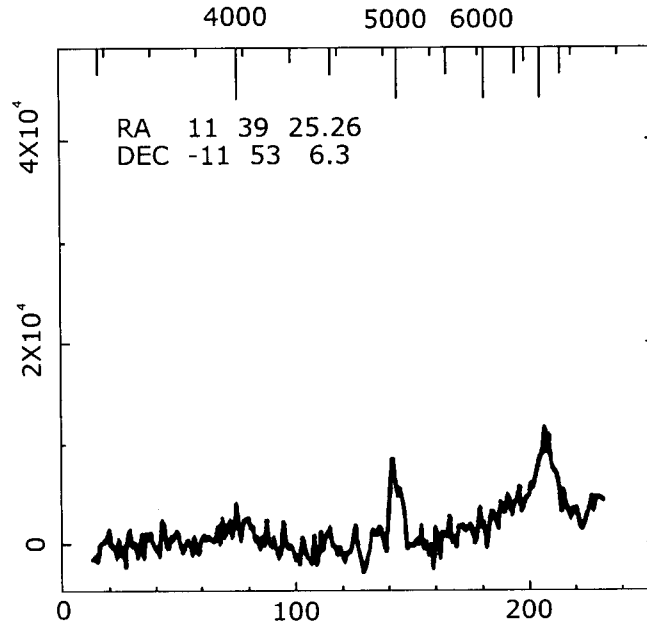


Fig. 1.— The objective-prism spectrum of 318-1 as a typical example. Upper and lower X-axes are, respectively, wavelength and pixel number. Y-axis represents the APM intensity on an arbitrary scale.

Then by comparing the coordinate of objects on direct R plate with the X,Y coordinate of prism objects, the coordinate of all prism objects are determined. For the transformation of two different coordinates on the direct plate and prism plate, a six parameter fitting was employed for the astrometric calibration.

The PPM (Proper Motion) Catalogue was used to select the astrometric standard stars on the direct R plate and about several hundred stars were adopted to determine RA and Dec of prism objects and the position accuracy within less than one arcsecond of the prism objects easily can be achieved. Then the one-dimensional objective-prism spectra for only the objects classified as a galaxy on direct plate were plotted on the monitor after the wavelength calibration. To do this the spectrum inside the box with a size of 50 by 256 pixels is taken and the total column intensity is calculated perpendicular to the dispersion direction. The size of the box is long enough to contain the longest and widest spectrum.

To find out the candidates of ELGs, the emission features of [OIII] $\lambda\lambda$ 4959,5007 and H_{β} 4861 were identified by eyeballing each spectrum one by one on a monitor. [OIII] $\lambda\lambda$ 4959,5007 and H_{β} emission lines were chosen because it was the selection criterion for the surveys of Moody, et al. (1988) that found most of the galaxies in the Bootes Void. For each field, spectra of more than 3000 objects classified as a galaxy on

direct R plate were searched to identify emission features. Among five differently classified types of all objects on direct R plate with stellar, noise, non-stellar, merged, and non-stellar and merged objects, only non-stellar objects were selected for spectral investigation as a galaxy. More or less evident emission features could be identified for about 30 to 40 galaxies varying from field to field.

The next criterion of ELGs were stronger emission features of [OIII] than H_{β} . And also the redshift amount of H_{β} and O[III] emission features were considered. Because the maximum redshift distance of probable galaxies inside the Hydra Void is about 10,000km s^{-1} , the maximum redshift amount of emission features should be less than 170Å. This amount of shift can be easily detected on each spectrum.

Our five fields are crowded with many objects. Therefore the high density of sources present on our plates and the number of spectra affected by the presence of a neighboring object is large. Due to this overlapping problem on our objective-prism plates, misidentification of emission features is inevitable in many cases. To reduce this, we compared the distance of emission features from the head of the spectra with the distance of an overlapping object from a candidate galaxy on the finding chart made with direct R plate. The redshift amount of about 170Å on a spectra at about 5000Å is equivalent to less than 10 pixels and

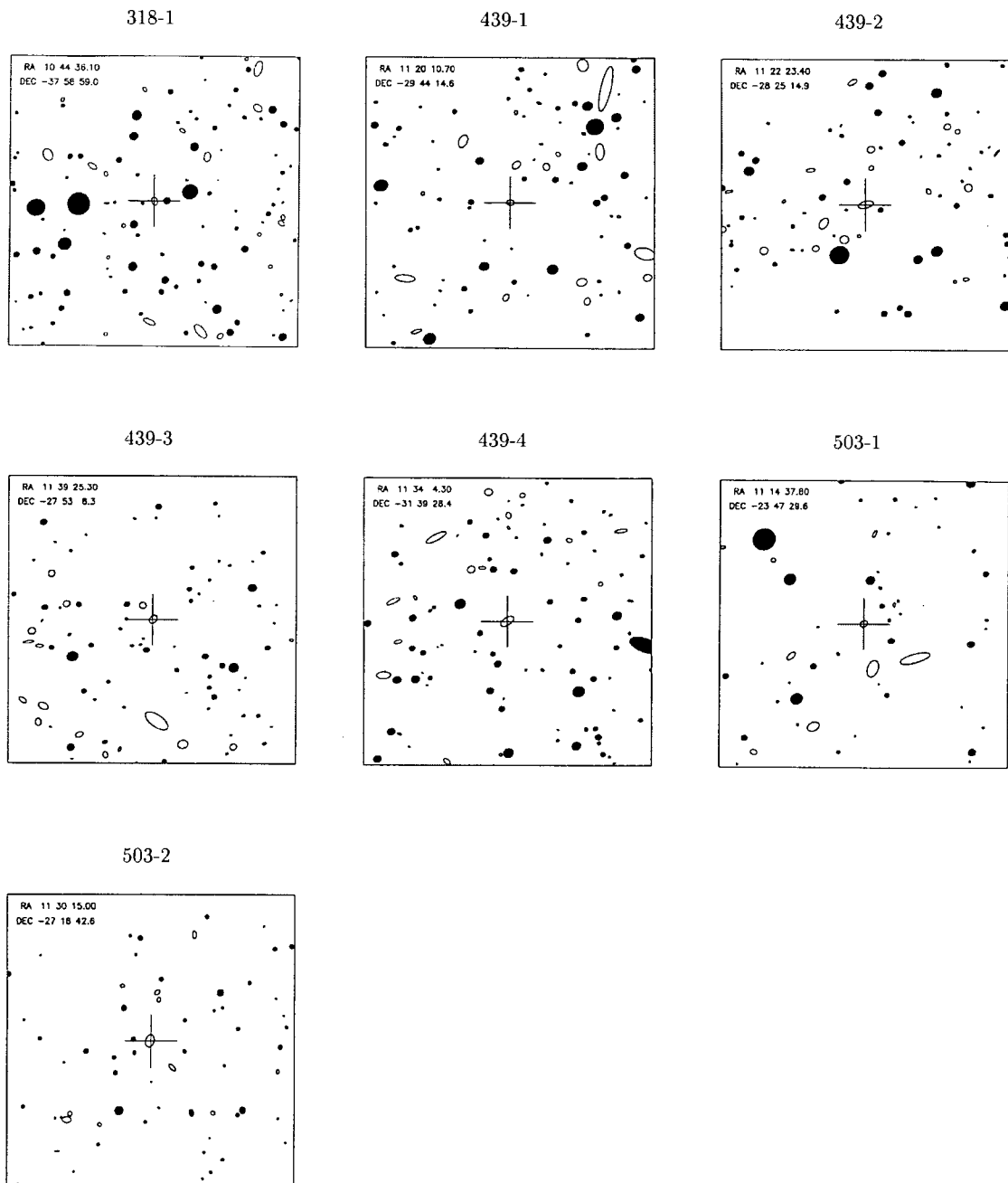


Fig. 2.— The charts of seven candidates of ELGs. The field of view of each chart is 5 arcmin \times 5 arcmin.

Table 2. List of the candidates of emission-line galaxies inside the Hydra Void

Name	RA(1950)	DEC(1950)	Mag(R)	Mag(B)
318-1	10 44 36.1	-37 58 59	16.59	17.24
439-1	11 20 10.7	-29 44 15	17.43	19.41
439-2	11 22 23.4	-28 25 15	14.42	16.18
439-3	11 39 25.3	-27 53 06	16.59	18.10
439-4	11 34 04.3	-31 39 28	15.41	15.23
503-1	11 14 37.8	-23 47 30	17.00	17.33
503-2	11 30 15.0	-27 18 43	?	14.05

this amount corresponds to about 13 arcsec on the direct R plate.

Therefore if an overlapping object is placed at around 90 arcsec along the dispersion direction from a candidate galaxy, we can not distinguish whether the emission feature is formed by an emission line or an overlapping object. Through these procedures we identified a total of 7 candidates of ELGs for five fields inside the Hydra Void and the list of the objects is presented in Table 2. Column 1 is the name of the objects where the first three digits indicate the field number. Column 2 and 3 are the coordinate of the objects, and column 4 and 5 are the red and blue magnitudes from the APM Catalogue.

We also present the spectrum of a candidate of 318-1 as typical example of all candidates of ELGs on Figure 1. In this figure, upper and lower X-axies are calibrated by wavelength and pixel number respectively. Y-axis represents the APM intensity on an arbitrary scale. RA and Dec of each object are given in the upper left corner of each panel. the finding charts from the red charts of the APM Catalogues for all candidates of ELGs are presented in Figure 2. The field view of the finding chart is 5 arcmin and the '+' symbol at the center marks the position of the candidate. The epoch of the coordinate displayed in the upper left corner is 1950.0, and upper and left correspond to the north and east. Filled circles are for stellar objects.

IV. CONCLUSION

Through the objective-prism search using the Tech Pan film, we identified a total of 7 candidates of ELGs for five fields inside the Hydra Void. If all 7 galaxies are really placed inside the Hydra Void and uniform distribution can be assumed, then about 0.04 ELGs per unit square degree can be calculated. Also if we assume spherical shape of the Bootes Void with the radius of 11 degrees, then the identified 27 ELGs lead the number distribution of about 0.07 galaxies per unit square degree.

Although direct comparison of the number of ELGs inside two different voids is difficult due to different methods of identification, number of ELGs inside the Hydra Void is crudely half inside the Bootes Void if

we again assume that all our 7 candidates are real Hydra galaxies. This big difference can be explained by the fact that either the average number of ELGs is not the same for different voids or, some candidate of faint ELGs were not detected in our search. Because there has been no study of the direct comparison of ELGs number for different void and, in addition, our five fields covered only 25% of total 20 fields of the Hydra Void, we can not reach any definite conclusion. It is, therefore, absolutely required to search the candidates of ELGs for all other fields of the Hydra Void for reliable direct comparison with the Bootes Void.

We wish to acknowledge the assistance given to this work by the staff members of the UKST at the Anglo-Australian Observatory. My thanks to Drs. A. Savage, M.J. Drinkwater, and S. Tritton for their collaborations in putting forward this project. Special thanks go to Dr. M. Irwin for scanning the prism films with the APM and providing the processed data with necessary software.

REFERENCES

- Cruzen, S.T., Weistrop, D., & Hoopes, C.G. 1997, AJ, 113, 1983
- Cruzen, S., Weistrop, D., Angione, R. & Hoopes, C. 1996, AAS, 189, 1402
- Dekel, A. & Silk, J. 1986, ApJ, 303, 39
- Dey, A., Strauss, M.A. & Huchra, J. 1990, AJ, 99, 463
- Dubinski, J., da Costa, L.N., Goldwirth, D.S., Lecar, M., & Piran, T. 1993, ApJ, 410, 458
- Fairall, A.P., Vettolani, G., & Chincârini, G. 1988, A&AS, 78, 269
- Hoffman, Y., Silk, J., & Wyse, R.F.G. 1992, ApJ, 388, L13
- Kim, C., Boller, Th, Ghosh, K.K, Swartz, D.A., & Ramsey, B.D. 2000, ApJL, accepted
- Kirshner, R.P., Oemler, A., Jr. & Schechter, P.L. 1981, ApJL, 248, 57
- Kirshner, R.P., Oemler, P., Schecter, P.L., & Sackett, S.A. 1987, ApJ, 314, 493
- Moody, J.W., & Kirshner, R.P. 1988, AJ, 95, 1629

- Phillipps, S. & Parker, Q.A. 1993, MNRAS, 265, 385
- Schwartzberg, J.M., Phillipps, S., Parker, Q.A. 1995, A&A, 293, 332
- Strauss, M.A. & Huchra, J. 1988, AJ, 95, 1602
- Tift, W.G., & Gregory, S.A. 1988, AJ, 95, 651
- van de Weygaert, R., & van Kampen, E. 1993, MNRAS, 263, 481
- Weistrop, D. 1994, in Violent Star Formation from 30 Doradus to QSOs, edited by G. Tenorio-Tengele (Cambridge University Press, Cambridge), p.100
- Willmer, C.N.A., da Costa, L.N., Pellegrini, P.S., Fairall, A.P., Latham, D.W., & Freudling, W. 1995, AJ, 109, 61